Received: 13 December 2021 | Revised: 19 March 2022 | Accepted: 26 April 2022

DOI: 10.4218/etrij.2021-0471

ORIGINAL ARTICLE

ETRI Journal WILEY

Co-located and space-shared multiple-input multiple-output antenna module and its applications in 12 × 12 multiple-input multiple-output systems

Longyue Qu[1] | **Haiyan Piao**[2] | **Guohui Dong**[3]

[1]School of Electronics and Information Engineering, Harbin Institute of Technology, Shenzhen, China

[2]Hanyang Antenna Design Co. Ltd., Shenzhen, China

[3]China United Network Communications Group Co. Ltd, Beijing, China

Correspondence
Longyue Qu, School of Electronics and Information Engineering, Harbin Institute of Technology, Shenzhen, China.
Email: rioinkorea@gmail.com

Funding information
This research was supported by Hanyang Antenna Design Co. Ltd., Shenzhen, China.

Abstract

In this study, we developed a co-located and space-shared multiple-input multiple-output (MIMO) antenna module with a modular design and high integration level. The proposed antenna pair includes a half-wavelength loop antenna and a dipole-type antenna printed on the front and back sides of a compact modular board. Owing to their modal orthogonality, these two independent antenna elements are highly self-isolated and free of additional decoupling components, even though they are assembled at the same location and within the same space. Thus, the proposed antenna is attractive in 5G MIMO systems. Furthermore, the proposed co-located and space-shared MIMO antenna module was employed in a 5G smartphone to verify their radiation and diversity performances. A 12 × 12 MIMO antenna system was simulated and fabricated using the proposed module. Based on the results, the proposed module can be employed in large-scale MIMO antenna systems for current and future terminal devices owing to its high integration, compactness, simple implementation, and inherent isolation.

KEYWORDS

5G MIMO, inherent isolation, MIMO antennas, modal orthogonality, modular design

1 | INTRODUCTION

Multiple-input multiple-output (MIMO) is a key technology that can remarkably increase the channel capacity and provide ultrahigh data rates for 5G applications [1–3]. By employing large-scale antenna elements in 5G devices, ultrahigh speed (up to multiple gigabits per second with a minimum user experienced data rate of one gigabit per second), low latency, and excellent reliability can be supported. Therefore, simple and feasible methods for the implementation of 5G MIMO technologies in wireless devices would promote the commercialization of veritable 5G services.

Within the 5G new radio spectrum, the sub-6-GHz band can achieve a better compromise between capacity and coverage than millimeter-wave bands. Thus, sub-6-GHz MIMO antenna systems in space-scarce terminal devices have attracted considerable attention since the allocation of the 3.5-GHz (3.4 GHz–3.6 GHz) band for 5G mobile communication [4].

TABLE 1 Comparison with the state of the art

References	Decoupling technique	Antenna allocation	Occupied volume	Isolation (dB)	−6 dB impedance bandwidth (MHz)	Cons and pros
[19]	Polarization control	Shared radiator	25 mm × 25 mm	>15	600	Need a large implementation area in the ground plane
[20]	Asymmetrical structure	Back-to-back	7 mm × 10 mm	>10	>200	(1) Require both the front and back sides of the ground plane (2) Do not support symmetrical structures
[21, 22]	Orthogonal current modes	Shared radiator	1 mm × 28.4 mm [21]; 1.5 mm × 25 mm [22]	>20	>200	(1) Suffer from difficult implementation (2) Need complex feeding network and rim cutting
[23, 24]	Current cancelation [23]; Mode control [24]	Edge-to-edge [23]; Shared space [24]	3 mm × 25.3 mm [23]; 4 mm × 20.6 mm [24]	>25	>270	Need large clearance areas
[25]	Complementary radiation patterns	Shared space	6.7 mm × 15.5 mm × 3.08 mm	>18	>200	Need vertically and horizontally three-dimensional structures
[26, 27]	Connection line	Connected radiator	7 mm × 30 mm [26]; 7.5 mm × 30 mm [27]	>10	>900	Large lateral distance and low isolation
[28, 29]	Modal orthogonality [28]; grounding branch [29]	Edge-to-edge	7 mm × 12 mm [28]; 7 mm × 22 mm [29]	>15	>200	(1) Require both the front and back sides of the ground plane (2) Do not support symmetrical structures
This work	Modal orthogonality	Shared space	4 mm × 22 mm	>16	>290	Modular design and reduced height

However, compact designs with high isolation (i.e., low mutual coupling) and low correlation have always been challenging issues, and the integration of large-scale antenna elements into the crowd terminal devices is of great interest. In the literature, decoupling and decorrelating techniques for MIMO antennas can be categorized into decoupling-component-based MIMO (neutralization lines, decoupling networks, parasitic elements, etc.) [5–14] and self-decoupled MIMO [15–29].

In decoupling-component-based MIMO, additional coupling paths created from decoupling components cancel out the original coupling path between antenna elements. However, extra occupation and complicated tuning efforts are often required to introduce these decoupling components; thus, compactness and integration are usually difficult to achieve. For example, using a closed-loop as the decoupling structure, two small ground-radiation antennas have been successfully decoupled, even though their edge-to-edge distance is only 1 mm [11]. However, the main disadvantage is their large clearance area, which limits their applications.

In self-decoupled MIMO, however, spatial distribution and polarization or pattern control are employed, preventing the time-consuming and case-by-case optimization efforts in the former technique. Although acceptable performance can be obtained through the spatial distribution of antenna elements, vast distances and large space areas are required [15–18]. Otherwise, polarization or radiation pattern control with self-decoupled performance is preferable. Related studies on this technique can be categorized into two. In the first category, two antenna elements are allocated, either edge-to-edge or connected [20,23,26–29]. In this way, a much closer distance and a tighter space have been achieved. The second category employs a shared radiator or shared space to achieve spatial reuse [19,21,22,24,25].

Herein, we assemble two independent antenna elements (a half-wavelength loop and a dipole-type antenna) into a singular modular board. One antenna element reuses the space the other one has occupied; thus, the two antenna elements overlap. Therefore, the two independent antenna elements have a shared space. Compared with previous reports [20,23,26–29], the proposed antenna requires less lateral space and occupies only one side of the ground plane. Compared with antennas that use a shared radiator [19,21,22], the proposed antenna can be controlled and constructed using a simpler method, and compared with those that employ shared space [24,25], the proposed antenna can achieve modular design without a large clearance area. Table 1 compares the proposed and state-of-the-art antennas to verify the novelty of the proposed technique.

The developed technique is simple and effective for co-located and space-shared MIMO antenna pairs, and its applications in MIMO systems were verified. The main contribution of this study is that two independent antenna elements are successfully assembled onto a compact and singular modular board without decoupling components, complicated excitation techniques, or specific construction processes.

The rest of this manuscript is organized as follows: Section 2 describes the proposed co-located and space-shared MIMO antenna module and its operation mechanism and presents various implementation cases to validate the feasibility and versatility of the proposed technique; Section 3 presents experiments and simulations on a 12 × 12 MIMO antenna array to demonstrate the feasibility of the proposed technique for 5G applications.

2 | CO-LOCATED AND SPACE-SHARED MIMO ANTENNA MODULE

2.1 | Antenna configuration

Figure 1 depicts the configuration of the proposed co-located and space-shared MIMO antenna module. A half-wavelength loop antenna (Antenna-1) and a dipole-type antenna (Antenna-2) are printed on the front and back sides of a modular board, respectively. Thus, two independent antenna elements are deployed in a singular and compact modular board, sharing the same space. The modular board has dimensions of 4 mm × 22 mm × 1 mm (0.047 λ × 0.257 λ × 0.012 λ) and is vertically installed along the edge of a 140 mm × 70 mm ground plane. Both the modular board and the ground plane are fabricated using a 1-mm-thick FR4 substrate ($\varepsilon_r = 4.4$, $\tan\delta = 0.02$). Notably, 1-mm ground clearance is reserved at the edge of the ground plane for easy installation of the modular board.

Antenna-1 is a widely used half-wavelength loop antenna and is printed on the front side of the modular board (yellow trace on the modular board). It is directly fed by a voltage source at one end and shorted to the ground plane at the other end. It has a symmetrically folded structure with an overall dimension of 4 mm × 18.8 mm (0.047 λ × 0.219 λ). Notably, half-wavelength loop antennas are widely used in various wireless devices owing to their simple structures, easy integration, and adjustable input impedance [30].

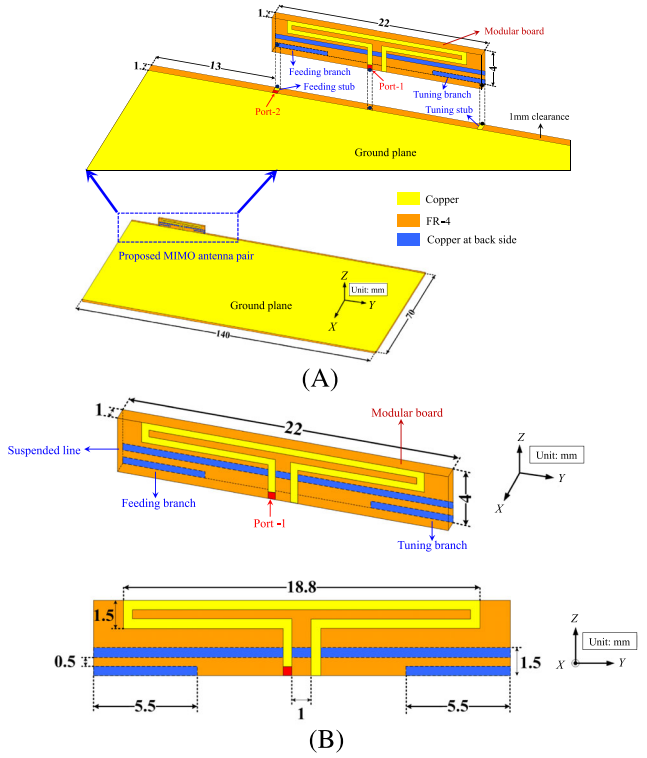

FIGURE 1 Configuration of the proposed MIMO antenna module: (A) perspective and (B) zoomed views of the modular board

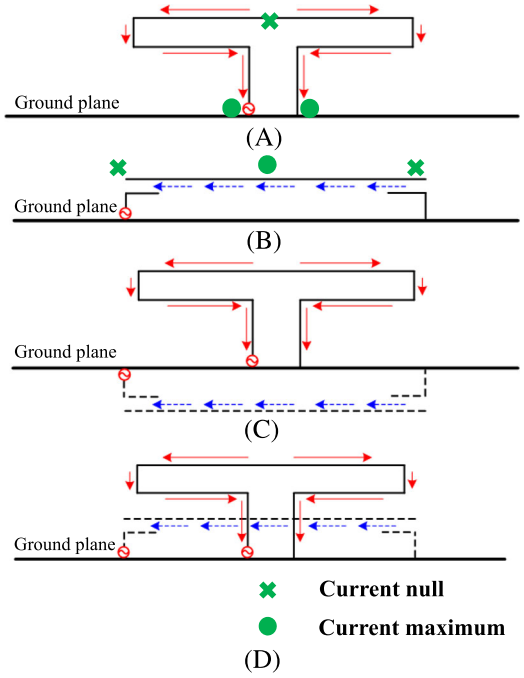

FIGURE 2 Schematic of the co-located and space-shared antenna pair with modal orthogonality: (A) loop-type current in Antenna-1; (B) dipole-type current in Antenna-2; (C) assembly method; (D) final assembly

Antenna-2 is a dipole-type antenna and is printed at the backside of the modular board (blue trace on the modular board). It consists of a suspended line for radiation, a feeding branch for impedance matching, and a tuning branch for easy resonance control. A feeding stub is printed on the ground clearance and connected to the feeding branch so that radiofrequency (RF) signals from a voltage source are fed into the suspended line. Thus, the feeding branch can capacitively excite the suspended line and control the input impedance of the antenna. Additionally, a tuning stub is printed on the ground clearance, connecting the ground plane and the tuning branch so that the tuning branch operates as a capacitive load to the suspended line, which enables resonance control without modifying the dimensions of the suspended line. Antenna-2 has overall dimensions of 1.5 mm × 22 mm × 1 mm (0.017 λ × 0.257 λ × 0.012 λ) and reuses the space behind Antenna-1, efficiently utilizing the limited volume of the modular board.

Schematic structures and the design process for the co-located and space-shared MIMO antenna pair are shown in Figure 2. The dominant current mode of Antenna-1 has current maxima at the two ends and current nulls at its center, equivalent to a vertically installed half-wavelength loop mode (Figure 2A), which is different from the one wavelength loop reported in [25]. Accordingly, the total electrical length L of Antenna-1 can be predetermined from the following equation:

$$f_r = \frac{1}{2L\sqrt{\varepsilon_r}}, \tag{1}$$

where f_r is the center operating frequency of the antenna and ε_r is the effective dielectric constant of the substrate. Therefore, the variables can be fine-tuned to further optimize Antenna-1. On the other hand, Antenna-2 is parallelly aligned with the ground plane and has current nulls at the two ends and current maxima at the center of the suspended line, resembling a horizontal dipole-type current mode (Figure 2B). The total electric length of the suspended line is one wavelength and can be designed using (1) to determine the initial length. Also, a tuning branch can be adopted for fine-tuning and optimization. A similar antenna was reported in [28]. The modal orthogonality enables the assembly of these two antenna elements on the upper and lower sides of the ground plane, sharing the same location (Figure 2C). This is similar to the report in [28], where both the front and back sides of the ground plane are occupied. Herein, however, owing to the structural compatibility of the

two antenna elements, the two independent antenna elements can be stacked together (Figure 2C), sharing the same location and space on the modular board.

2.2 | Simulation results and operation mechanism

Figure 3 shows the simulated scattering parameters (*S*-parameters) for the proposed antenna pair. Wideband impedance bandwidths and high isolation properties were obtained. As shown in the S_{11} and S_{22} curves, the 3:1 VSWR bandwidths of Antenna-1 and Antenna-2 are 370 MHz (from 3.3 GHz to 3.67 GHz) and 290 MHz (from 3.36 GHz to 3.65 GHz), respectively, fully covering the 3.5-GHz operating band. As observed in the S_{12} curve, the isolation within the target frequency band is higher than 16 dB, indicating that the proposed co-located and space-shared MIMO antenna module is highly self-isolated without the need for decoupling components, complex excitation techniques, or special manufacturing processes.

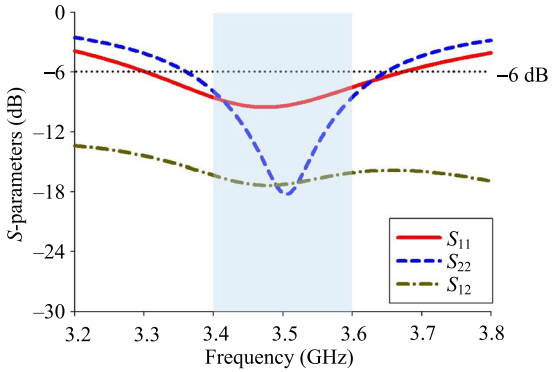

FIGURE 3 Simulated scattering parameters (*S*-parameters) for the proposed MIMO antenna module

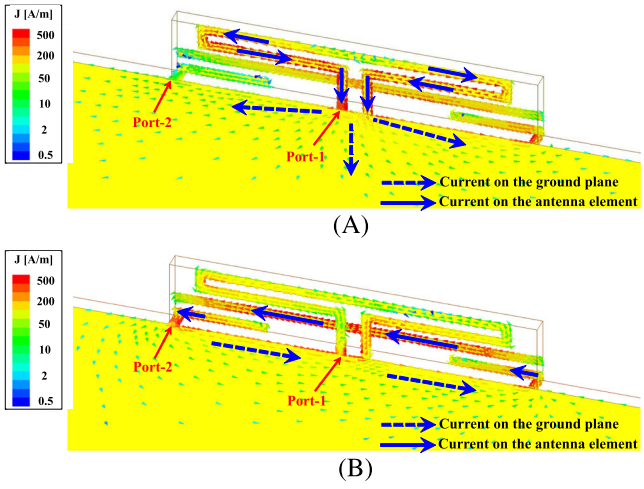

FIGURE 4 Simulated surface current distributions with the excitation of (A) Port 1 and (B) Port 2

The simulated surface current distributions at 3.5 GHz are shown in Figure 4 to further verify the operation mechanism of the proposed technique. When Antenna-1 is excited (Figure 4A), strong currents flow at the two ends of the antenna structure and spread into the ground plane, whereas current nulls are produced at the center of the antenna structure. As shown in Figure 4B, when Antenna-2 is excited, a dipole-type current mode is generated in the suspended line, whereas inverse current flows are distributed along the edge of the ground plane. Even when the dipole-type antenna is quite close to the ground plane, the current distribution over the ground plane is weak, which promotes antenna radiation performance. Accordingly, not only the current modes in the two antenna elements but also the current distributions over the ground plane are orthogonal to each other. Thus, extremely weak currents are induced from one port to another, resulting in their high port-to-port isolation property.

2.3 | Further study and discussion

Herein, we discuss alternative implementation cases for the proposed technique, as shown in Figure 5.

The proposed antenna pair (Figure 1) is derived from Case 1 (Figure 5A), where a simple center-fed external dipole antenna (dashed trace) is placed behind the half-wavelength loop antenna. The S-parameters show that the external dipole antenna is not perfectly impedance-matched because it is too closely arranged along the edge of the ground plane, resulting in a low impedance characteristic. Nevertheless, there is high isolation between the two antenna elements. To confirm this behavior in Case 1, the center-fed external dipole antenna was impedance-matched by adopting a feeding line, as shown in Case 2 (Figure 5B). In this way, both antenna elements become impedance-matched and highly isolated.

The external dipole antennas in Cases 1 and 2 may not be easily fed by a voltage source from the ground plane (i.e., the main board of the wireless devices). Therefore, we developed alternative excitation methods, such as the capacitive coupling method in Figure 1 and the inductive coupling method in Figure 5C (Case 3), for practical application scenarios. In Case 3, a loop-type feeding structure, located at the current maxima of the suspended line, is formed by connecting a voltage source at one end and the ground plane at the other end to magnetically excite the suspended line as a dipole-type

antenna. The results of Case 3 are similar to those in Figure 3 and Case 2. Therefore, the proposed technique is a simple method that can achieve full integration and inherent isolation simultaneously, regardless of the excitation method.

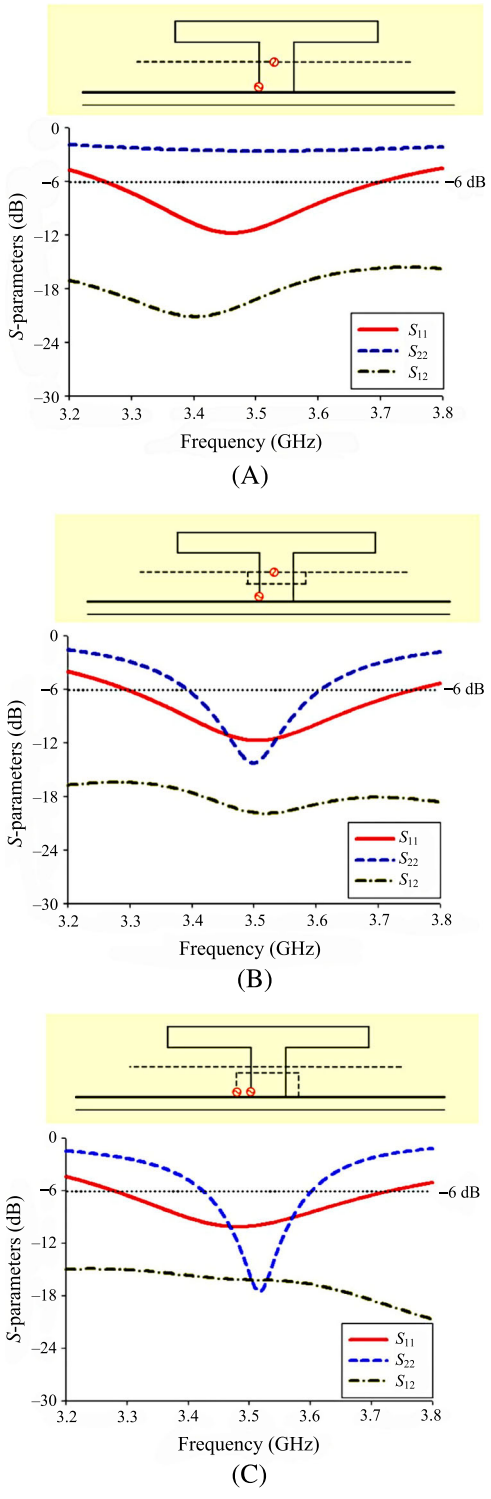

FIGURE 5 Various implementation cases for the proposed MIMO antenna pair: (A) Case 1, (B) Case 2, and (C) Case 3

3 | 12 × 12 MIMO ANTENNA SYSTEM

In this section, a large-scale MIMO antenna system is demonstrated by employing the developed MIMO antenna module to show its applicability in terminal devices. A popularly used smartphone is used as a platform for 5G scenarios, and a 12 × 12 MIMO antenna system is established as a case study.

3.1 | MIMO antenna configurations

Figure 6A shows a 140 mm × 70 mm ground plane used to model a currently used 5G smartphone. In the industry, 3G/4G antenna systems will coexist with 5G systems for a long time and are usually imposed at the upper and lower ends of smartphones. Therefore, we allocated the proposed 12 × 12 MIMO antennas for 5G applications along the long sides of the ground plane to simulate the practical scenarios. Accordingly, six sets of the proposed MIMO antenna module were used to construct a 12 × 12 MIMO antenna system (Figure 6A,B).

3.2 | Simulation and measurement results

This subsection presents the simulated and measured results of the proposed 12 × 12 MIMO antennas to verify

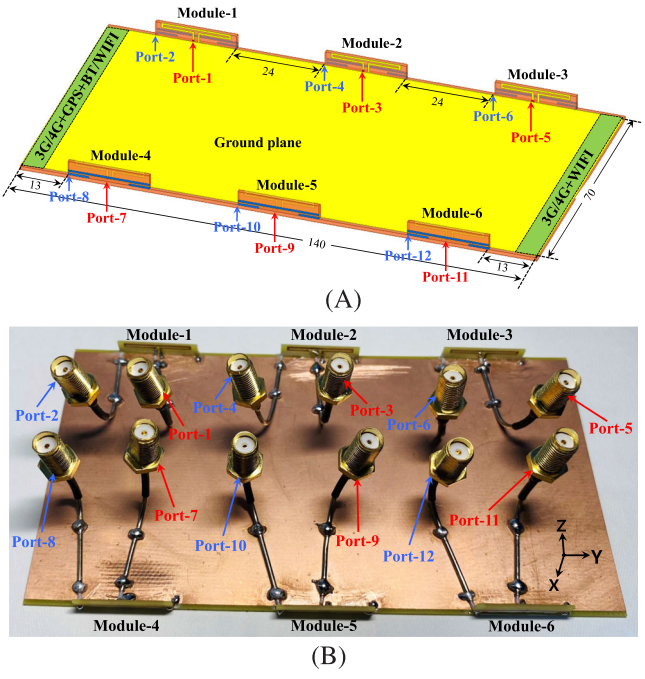

FIGURE 6 12 × 12 MIMO antenna system for 5G applications: (A) simulation model and (B) fabricated system

the feasibility of the proposed technique. The simulation model was built in HFSS 19, and the fabrication was tested using a network analyzer and measured in a 6 m × 3 m × 3 m three-dimensional (3D) CTIA OTA anechoic chamber.

Figure 7 shows the simulated and measured S-parameters for the proposed 12 × 12 MIMO antennas. As shown in Figure 7A, the S_{11} and S_{22} curves fully cover the 3.5-GHz operation band for 5G applications, and the mutual coupling between them (S_{12}) is lower than −17 dB. The measurement results agree well with the simulation with only a minor discrepancy, which is attributed to the fabrication errors and implementation accuracy. Meanwhile, the isolation between any two antenna elements is more than 16 dB, as shown by the measured transmission coefficients in Figure 7B,C. This satisfies the engineering requirements for industrial applications.

The measured total efficiencies are shown in Figure 8. Both Antenna-1 and Antenna-2 showed high efficiencies greater than 60% within the operation band, indicating high radiation performance and their feasibility in practical applications. The antenna elements in all six modules (Figure 6B) showed similar radiation efficiencies; thus, only the efficiency curves of Antenna-1 and Antenna-2 in Module-1 are shown herein for

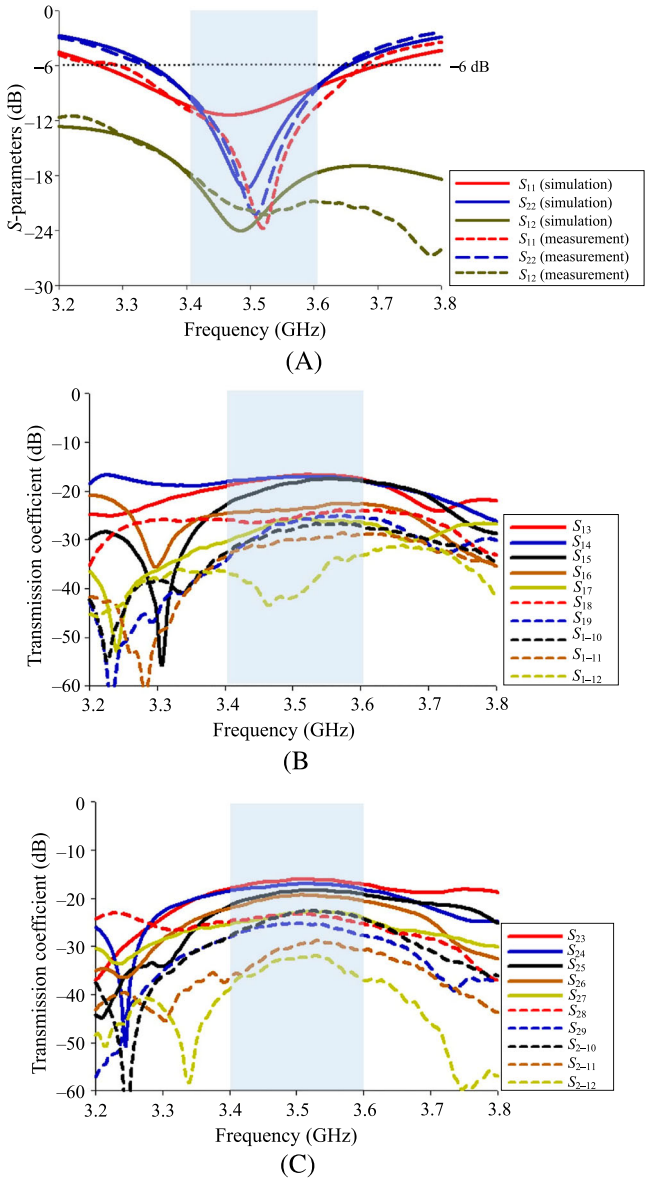

FIGURE 7 Simulated and measured results: (A) S-parameters; (B) and (C) measured transmission coefficients

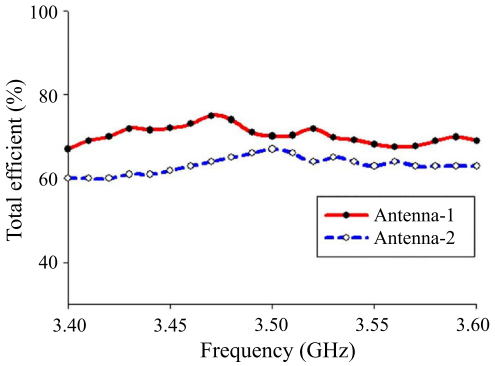

FIGURE 8 Measured total efficiencies

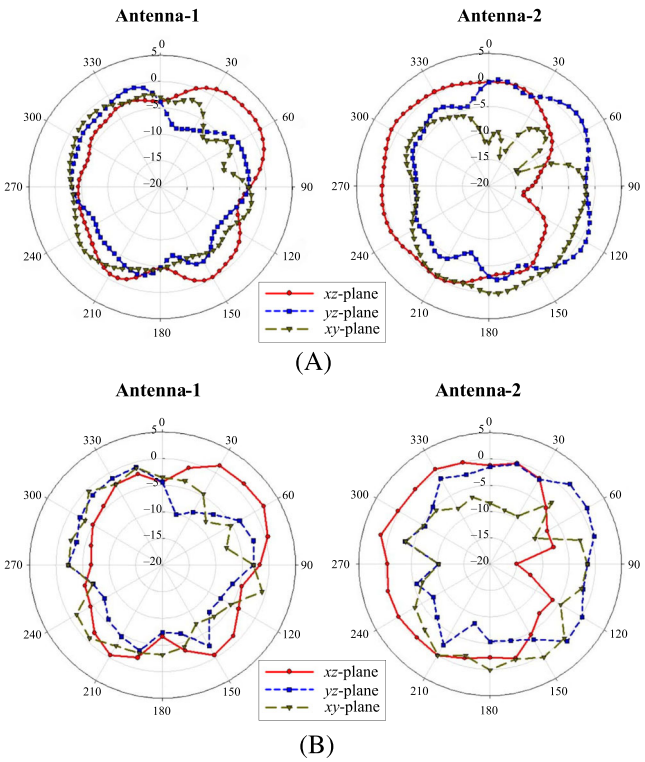

FIGURE 9 (A) Simulated and (B) measured radiation patterns at 3.5 GHz

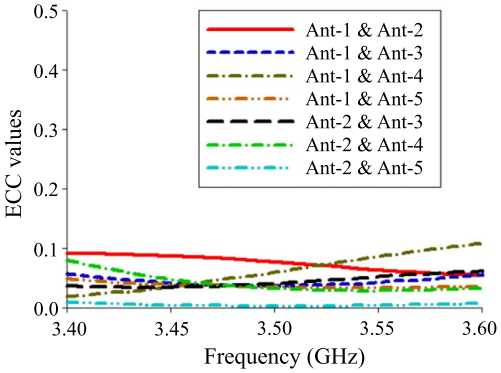

FIGURE 10 Measured envelope correlation coefficients of the fabricated 12 × 12 MIMO antennas

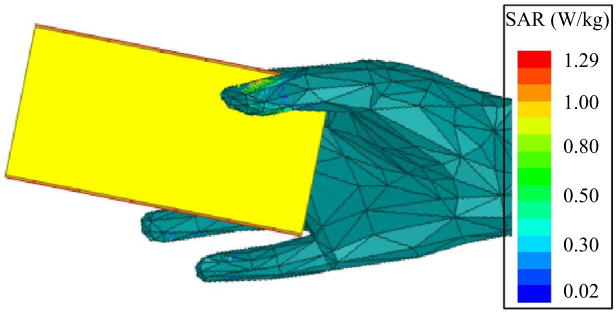

FIGURE 11 Simulation model for the specific absorption rate based on a user's hand at 3.5 GHz

simplicity. Figure 9 shows the radiation patterns obtained at 3.5 GHz in *xz*-, *yz*-, and *xy*-planes. Antenna-1 and Antenna-2 showed approximately complementary radiation patterns, and their maximum gains oppose each other, which is desired for signal reception. Correlation is a critical parameter to evaluate the diversity of MIMO antennas and is calculated from the vector properties (amplitude, phase, and polarization) of the complex 3D far-field radiation patterns [31]. Accordingly, herein, envelope correlation coefficients (ECCs) ρ_e were derived (Figure 10), and their values are all below 0.1, which is way lower than the acceptable limit (0.5) in mobile communications. In conclusion, the proposed technique is a simple yet efficient method with high inherent isolation, extraordinary diversity performance, extremely high integration, and very simple implementation, making it suitable for 5G MIMO applications in current and future terminal devices.

The specific absorption rate (SAR) is an important parameter for evaluating human exposure to electromagnetic waves during data transceiving and should be as low as possible [32]. Herein, we developed a SAR simulation model based on a user's right-hand phantom using a full-wave simulator (Figure 11). At 3.5 GHz, the peak SAR was 1.29 W/kg, which is lower than the SAR limit (1.6 W/kg) for 1 g of tissue.

4 | CONCLUSION

In this study, we developed a co-located and space-shared MIMO antenna module by fully integrating two independent antenna elements in a compact and singular modular board. The advantages of the proposed technique include the modular design and high integration level owing to the spatial reuse, which is attributed to the modal orthogonality and structural compatibility of the half-wavelength loop and dipole-type antennas. Thus, inherent isolation and diversity performance are achieved even when these two independent antenna elements are integrated within a shared volume. A 12 × 12 MIMO antenna system with six sets of modular boards was simulated and fabricated to verify the feasibility of the proposed technique in large-scale MIMO applications for current and future terminal devices. High isolation (>16 dB), high radiation efficiency (>60%), and low ECC (<0.1) were measured. In our future studies, we shall investigate spatial-reused wideband and multiband antenna pairs.

CONFLICT OF INTEREST

The authors declare that there are no conflicts of interest.

ORCID

Longyue Qu https://orcid.org/0000-0001-5152-091X

REFERENCES

1. F. Boccardi, R. W. Heath, A. Lozano, T. L. Marzetta, and P. Popovski, *Five disruptive technology directions for 5G*, IEEE Commun. Mag. **52** (2014), no. 2, 74–80.
2. E. Björnson, E. G. Larsson, and T. L. Marzetta, *Massive MIMO: ten myths and one critical question*, IEEE Commun. Mag. **54** (2016), no. 2, 114–123.
3. A. Al-Wahhamy, H. Al-Rizzo, and N. E. Buris, *Efficient evaluation of massive MIMO channel capacity*, IEEE Syst. J. **14** (2020), no. 1, 614–620.
4. WRC-15 Press Release, *World Radiocommunication Conference allocates spectrum for future innovation*. Available from: http://www.itu.int/net/pressoffice/press_releases/2015/56.aspx [last accesed November 2015].
5. S. W. Su, C. T. Lee, and S. C. Chen, *Very-low-profile, triband, two-antenna system for WLAN notebook computers*, IEEE Antennas Wirel. Propag. Lett. **17** (2018), no. 9, 1626–1629.
6. M. Wang, B. Xu, Y. Li, Y. Luo, H. Zou, and G. Yang, *Multiband multiple-input multiple-output antenna with high isolation for future 5G smartphone applications*, Int. J. RF Microw. Comput. Aid. Eng. **29** (2019), no. 7, e21758.

7. Y. Li, C.-Y. D. Sim, Y. Luo, and G. Yang, *Metal-frame-integrated eight-element multiple-input multiple-output antenna array in the long term evolution bands 41/42/43 for fifth generation smartphones*, Int. J. RF Microw. Comput. Aid. Eng. **29** (2019), no. 1, e21495.
8. Y. Li, C. Y. D. Sim, Y. Luo, and G. Yang, *4G/5G multiple antennas for future multi-mode smartphone applications*, IEEE Access **6** (2019), no. 2019, 28041–28053.
9. D. Serghiou, M. Khalily, V. Singh, A. Araghi, and R. Tafazolli, *Sub-6 GHz dual-band 8 × 8 MIMO antenna for 5G smartphones*, IEEE Antennas Wirel. Propag. Lett. **19** (2020), no. 9, 1546–1550.
10. C. Deng, *Compact broadband multi-input multi-output antenna covering 3300 to 6000 MHz band for 5G mobile terminal applications*, Microw. Opt. Technol. Lett. **62** (2020), no. 10, 1–7.
11. H. Piao, Y. Jin, Y. Xu, and L. Qu, *MIMO ground-radiation antennas using a novel closed-decoupling-loop for 5G applications*, IEEE Access **8** (2020), 142714–142724.
12. Z. Xu and C. Deng, *High-isolated MIMO antenna design based on pattern diversity for 5G mobile terminals*, IEEE Antennas Wirel. Propag. Lett **19** (2020), no. 3, 467–471.
13. Y. Q. Hei, J. G. He, and W. T. Li, *Wideband decoupled 8-element MIMO antenna for 5G mobile terminal applications*, IEEE Antennas Wirel. Propag. Lett **20** (2021), no. 8, 1448–1452.
14. M. Y. Li, Y. L. Ban, Z.-Q. Xu, J. Guo, and Z.-F. Yu, *Tri-polarized 12-antenna MIMO array for future 5G smartphone applications*, IEEE Access **6** (2018), 6160–6170.
15. Y. Liu, A. Ren, H. Liu, H. Wang, and C. Y. D. Sim, *Eight-port MIMO array using characteristic mode theory for 5G smartphone applications*, IEEE Access **7** (2019), 45679–45692.
16. C.-Y. D. Sim, H. Y. Liu, and C. J. Huang, *Wideband MIMO antenna array design for future mobile devices operating in the 5G NR frequency bands n77/n78/n79 and LTE Band 46*, IEEE Antennas Wirel. Propag. Lett. **19** (2020), no. 1, 74–78.
17. A. Zhao and Z. Ren, *Size reduction of self-isolated MIMO antenna system for 5G mobile phone applications*, IEEE Antennas Wirel. Propag. Lett. **18** (2019), no. 1, 152–156.
18. M.-Y. Li, Y.-L. Ban, Z.-Q. Xu, G. Wu, C.-Y.-D. Sim, K. Kang, and Z.-F. Yu, *Eight-port orthogonally dual-polarized antenna array for 5G smartphone applications*, IEEE Trans. Antennas Propag. **64** (2016), no. 9, 3820–3830.
19. N. O. Parchin, Y. I. A. Al-Yasir, A. H. Ali, I. Elfergani, J. M. Noras, J. Rodriguez, and R. A. Abd-Alhameed, *Eight-element dual-polarized MIMO slot antenna system for 5G smartphone applications*, IEEE Access **7** (2019), 15612–15622.
20. K.-L. Wong, C.-Y. Tsai, and J.-Y. Lu, *Two asymmetrically mirrored gap-coupled loop antennas as a compact building block for eight-antenna MIMO array in the future smartphone*, IEEE Trans. Antennas Propag. **65** (2017), no. 4, 1765–1778.
21. A. Ren, Y. Liu, and C.-Y. Sim, *A compact building block with two shared-aperture antennas for eight-antenna MIMO array in metal-rimmed smartphone*, IEEE Trans. Antennas Propag. **67** (2019), no. 10, 6430–6438.
22. L. Chang, Y. Yu, K. Wei, and H. Wang, *Polarization-orthogonal co-frequency dual antenna pair suitable for 5G MIMO smartphone with metallic bezels*, IEEE Trans. Antennas Propag. **67** (2019), no. 8, 5212–5220.
23. H. Piao, Y. Jin, and L. Qu, *Isolated ground-radiation antenna with inherent decoupling effect and its applications in 5G MIMO antenna array*, IEEE Access **8** (2020), 139892–139902.
24. H. Piao, Y. Jin, and L. Qu, *A compact and straightforward self-decoupled MIMO antenna system for 5G applications*, IEEE Access **8** (2020), 129236–129245.
25. C.-Z. Han, L. Xiao, Z. Chen, and T. Yuan, *Co-located self-neutralized handset antenna pairs with complementary radiation patterns for 5G MIMO applications*, IEEE Access **8** (2020), 73151–73163.
26. X.-T. Yuan, Z. Chen, T. Gu, and T. Yuan, *A wideband PIFA-pair-based MIMO antenna for 5G smartphones*, IEEE Antennas Wirel. Propag. Lett. **20** (2021), no. 3, 371–375.
27. L. Sun, Y. Li, Z. Zhang, and H. Wang, *Self-decoupled MIMO antenna pair with shared radiator for 5G smartphones*, IEEE Trans. Antennas Propag. **68** (2020), no. 5, 3423–3432.
28. L. Sun, H. Feng, Y. Li, and Z. Zhang, *Compact 5G MIMO mobile phone antennas with tightly arranged orthogonal-mode pairs*, IEEE Trans. Antennas Propag. **66** (2018), no. 11, 6364–6369.
29. Z. Ren and A. Zhao, *Dual-band MIMO antenna with compact self-decoupled antenna pairs for 5G mobile applications*, IEEE Access **7** (2019), 82288–82296.
30. A. Constantine, *Balanis, antenna theory: analysis and design*, 4th ed., John Wiley & Sons, 2016.
31. R. G. Vaughan and J. B. Andersen, *Antenna diversity in mobile communications*, IEEE Trans. Veh. Technol. **36** (1987), 149–172.
32. C95. *1-2019 - IEEE Standard for Safety Levels with Respect to Human Exposure to Electric, Magnetic, and Electromagnetic Fields, 0 Hz to 300 GHz*. Available from: https://standards.ieee.org/standard/C95_1-2019.html. [last accessed: June 2020].

AUTHOR BIOGRAPHIES

Longyue Qu received the MS and PhD degrees in electromagnetics and microwave engineering from the Hanyang University, Seoul, Republic of Korea, in 2015 and 2018, respectively. He was a post-doctoral researcher at Hanyang University from September 2018 to August 2019 and then was promoted as an Assistant Research Professor. From 2019 to 2022, he was a co-founder and CTO of Hanyang Antenna Design Co. Ltd, Shenzhen, China. Since 2022, he has been an Assistant Professor with the School of Electronics and Information Engineering, Harbin Institute of Technology, Shenzhen, China. He is the author of more than 40 articles and more than 30 inventions. He serves as a reviewer for several international journals and conferences. He also serves as an Editorial Board Member in the *International Journal of Sensors, Wireless Communications and Control*. His current research interests include

antenna theory and design, metamaterial-based antenna technology, millimeter-wave arrays, and RF circuits. Dr. Qu was a recipient of the Korean Government Scholarship Award and China Scholarship Council (CSC). His research is listed in the Top 100 National R&D Excellence Award in 2015.

Haiyan Piao received the BSc degree in Communication Engineering from Yanbian University, China, in 2013, and the MSc degree from the Department of Microwave Engineering, Hanyang University, Seoul, South Korea, in 2017. She is currently a senior engineer at Hanyang Antenna Design Co. Ltd, Shenzhen, China. Her expertise is antennas for MIMO, 5G communications, and the IoT devices.

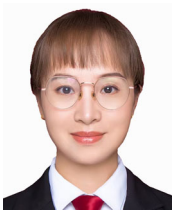

Guohui Dong is currently a senior technician in China United Network Communications Group Co., Ltd, China. Her expertise is communication systems.

How to cite this article: L. Qu, H. Piao, and G. Dong, *Co-located and space-shared multiple-input multiple-output antenna module and its applications in 12 × 12 multiple-input multiple-output systems*, ETRI Journal **45** (2023), 203–212. https://doi.org/10.4218/etrij.2021-0471